



HAL
open science

**Film-blown blends of
poly(3-hydroxybutyrate-co-3-hydroxyvalerate) by
compatibilization with
poly(butylene-co-succinate-co-adipate) with a free
radical initiator**

Benjamin Le Delliou, Olivier Vitrac, Anir Benihya, Patrice Dole, Sandra
Domenek

► **To cite this version:**

Benjamin Le Delliou, Olivier Vitrac, Anir Benihya, Patrice Dole, Sandra Domenek. Film-blown blends of poly(3-hydroxybutyrate-co-3-hydroxyvalerate) by compatibilization with poly(butylene-co-succinate-co-adipate) with a free radical initiator. *Polymer Testing*, 2023, 124, pp.108072. 10.1016/j.polymertesting.2023.108072 . hal-04420432

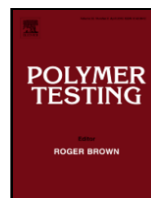
HAL Id: hal-04420432

<https://hal.science/hal-04420432>

Submitted on 26 Jan 2024

HAL is a multi-disciplinary open access archive for the deposit and dissemination of scientific research documents, whether they are published or not. The documents may come from teaching and research institutions in France or abroad, or from public or private research centers.

L'archive ouverte pluridisciplinaire **HAL**, est destinée au dépôt et à la diffusion de documents scientifiques de niveau recherche, publiés ou non, émanant des établissements d'enseignement et de recherche français ou étrangers, des laboratoires publics ou privés.



Film-blown blends of poly(3-hydroxybutyrate-co-3-hydroxyvalerate) by compatibilization with poly(butylene-co-succinate-co-adipate) with a free radical initiator

Benjamin Le Delliou^a, Olivier Vitrac^a, Anir Benihya^a, Patrice Dole^b, Sandra Domenek^{a,*}

^a UMR 0782 SayFood Paris-Saclay Food and Bioproduct Engineering Research Unit, INRAE, AgroParisTech, Université Paris-Saclay, 91120, Palaiseau, France

^b CTCPA Centre Technique de la Conservation des Produits Agricoles, Bourg-En-Bresse, France

ARTICLE INFO

Keywords:

Polymer processing
Film blowing
Biobased polymers
Biodegradable polymers
Food packaging
Mechanical stability
Compatibilizer

ABSTRACT

Poly(3-hydroxybutyrate-co-3-hydroxyvalerate) (PHBV) is a sustainable and biodegradable polymer that has potential for use in food packaging. However, its low melt strength makes it difficult to process using film-blowing techniques. To address this issue, 70% PHBV and 30% poly(butylene-co-succinate-co-adipate) (PBSA) were blended with dicumyl peroxide (DCP) as a compatibilizer. The resulting blend showed crosslinking and the presence of long-branched structures, as evidenced by Cole-Cole and van-Gurp-Palmen plots. The optimum formulation (30% PBSA and 0.1 phr DCP) improved the melt flow index, reducing it from 90 g/10 min (neat PHBV) to 22 g/10 min. This allowed for the successful small-scale production of blown PHBV/PBSA films. The thermal properties of PHBV, such as the glass transition and crystallinity index, remained unchanged with the addition of DCP. The films displayed a brittle behavior and a lower modulus compared to neat PHBV. However, they could be heat-sealed, and their mechanical properties remained stable during a six-month storage experiment under freezer conditions. Overall, the compatibilized PHBV/PBSA blend shows potential for use in the production of packaging films through film blowing.

1. Introduction

The food packaging industry faces a significant challenge in increasing the sustainability of polymers and reducing plastic pollution. To decrease the impact of food packaging, the development of bio-based and biodegradable materials that meet the necessary performance standards for food storage and protection is crucial. Polyhydroxyalkanoates (PHAs) are a promising solution, as they are thermoplastic polyesters produced by microorganisms as a form of carbon and energy storage in response to limited resources in the culture medium [1]. PHAs are 100% bio-based and biodegradable [1,2], and short-chain-length PHAs such as poly(3-hydroxybutyrate) (PHB) and poly(3-hydroxybutyrate-co-3-hydroxyvalerate) (PHBV) are already available commercially. PHBV is the most commonly produced PHA and can be produced using waste from agriculture and food industries [3–7], promoting a circular economy. However, PHBV has limitations such as its stiff, brittle, and highly crystalline nature, with a typical elongation at break of less than 5% and a stress at break of 30–40 MPa. Its glass transition temperature (T_g) ranges between 0 and 5 °C and it is subject to secondary crystallization during storage [1]. Additionally, PHBV has a narrow processing

window due to its thermal degradation temperature measured by thermogravimetry under N₂ (260 °C) being close to its melting temperature of around 170 °C [8]. As a comparison, the thermal degradation temperature under nitrogen of low-density polyethylene, which is commonly used for flexible food packaging is approximately 320 °C and its processing is possible starting with its plasticizing temperature around 160 °C [9].

Despite the significant research effort to develop PHBV-based materials for food packaging, there is a scarcity of reports on thermal processing techniques that can be scaled for industrial production [7]. PHBV has a low melt strength and viscosity [1], which is advantageous for the production of articles like trays through injection molding. However, most food packaging uses flexible films, which are typically produced by film-blowing extrusion, a processing method that requires high melt strength and extensional viscosity. Few studies are reporting successful film blowing of PHBV [7]. One strategy to overcome the limitations of PHBV is to use a multilayer architecture with an auxiliary polymer, such as poly(butylene-co-adipate-co-terephthalate) (PBAT), during film blowing [10–12]. This approach has shown to provide acceptable bubble stability and improved film toughness. As an illustra-

* Corresponding author. AgroParisTech, 22 place de l'Agronomie, 91120, Palaiseau, France.

E-mail address: sandra.domenek@agroparistech.fr (S. Domenek).

<https://doi.org/10.1016/j.polymeresting.2023.108072>

Received 14 February 2023; Received in revised form 7 May 2023; Accepted 18 May 2023
0142-9418/© 20XX

tion, using PHBV as the inner layer increases the elongation at break by 358–539% compared to 11–19% when it is used as the outer layers [11]. The use of a compatibilizer, such as dicumyl peroxide (DCP), can also improve the melt viscosity and interfacial adhesion of the polymers in polymer blends [13,14]. Ma et al. [15] proposed that DCP induces radicals on the different macromolecular chains. Crosslinking between both polymers can thus occur by a radical combination reaction. This would be possible at the interface and inside a given polymer phase. This has allowed for the decrease in film thickness and increase in PHBV content to a maximum of 50 wt% [12]. An alternative strategy is to blend PHBV with a second polymer and use film-blowing extrusion to produce PHBV films [12,16–19]. This approach has been successful in improving bubble stability and increasing the PHBV content potentially higher than 50 wt%. Films with 70 wt% PHBV have been produced using PBAT or poly(butylene sebacate-co-butylene terephthalate) [12].

An alternative to the mostly petrochemical PBAT (except adipate, which can be obtained from renewable resources) is the aliphatic, biodegradable, and partially or totally biobased polyester poly(butylene-co-succinate-co-adipate) (PBSA). All three monomer units can be obtained from renewable resources [20]. PBSA has a low glass transition temperature ($-45\text{ }^{\circ}\text{C}$), high elongation at break ($>200\%$), and high melt strength [8]. Extensive research has been conducted on the compatibilization of blends of poly(lactic acid) (PLA) and PBSA using chain extenders [21–25]. For example, Eslami and Kamal [23] showed that blends containing a multifunctional chain extender (named CESA) increased elongational viscosity and melt strain-hardening behavior. Chain extension and branching and increased viscosity are positive for film blowing extrusion, as demonstrated by Mallet et al. [26] for the case of PLA. The use of chain extenders is furthermore positive for tensile properties. For example, the addition of 0.5 phr epoxy styrene-acrylic oligomer increased the elongation at break of PLA/PBSA blends by a factor 4 [24].

In our previous study [8], the characteristics of PHBV/PBSA blends were analyzed, and the optimal blend composition was determined based on melt viscosity and mechanical properties, which was found to be 70/30 wt% PHBV/PBSA. However, the mechanical properties were limited by the brittleness of PHBV, with an elongation at break as low as 3% even with a PBSA content of 70 wt%. The stress at break indicated that the rupture was likely occurring at the PHBV/PBSA interfaces, as it was lower than the stress at break of pure PHBV in all cases.

In this study, we present the development of compatibilized PHBV/PBSA blends using DCP, which can be processed through film blowing. For that, we used a small-scale film blowing extrusion equipment. The morphological, rheological, thermal, and mechanical properties of the blends and blown films were characterized, and their performance in the target application was evaluated. Packaging tests and aging studies were conducted under frozen food service conditions, and the behavior of the films in contact with food was assessed.

2. Materials and methods

2.1. Materials

Commercial PHBV (PHI 002) and PBSA (PBE 001) were purchased from NaturePlast (France). Two different batches of PHBV were used in the work, one for the development of the formulation using the batch mixer and the other for twin screw extrusion and film blowing extrusion with the optimized blend composition. A ^1H NMR analysis of PHBV was carried out, the calculated ratio of 3-hydroxybutyrate over 3-hydroxyvalerate was 100 (1 mol% HV). Dicumyl peroxide was purchased from ACROS and used as received.

2.2. Compatibilized polymer blends

2.2.1. Batch mixing

Polymers were dried at $70\text{ }^{\circ}\text{C}$ under vacuum for at least 6 h before use. Compatibilized PHBV/PBSA 70/30 blends with DCP contents of 0, 0.02, 0.1, 0.2, and 1.0 phr (parts per hundred of resin on a weight basis, meaning that 0.02 phr correspond to 100 g blend + 0.02 g DCP) were melt-blended in the internal mixer SCAMEX Rheoscam (France) at $190\text{ }^{\circ}\text{C}$ and 90 rpm for 9 min. PHBV was pre-melted for 6 min. The pre-melting was necessary to reach a homogenous blend. Then, PBSA pellets mixed with DCP were introduced and mixed for 3 min. The blended materials were pulled out of the mixing chamber and air-dried. They were stored in a desiccator over silica gel.

2.2.2. Twin screw extrusion (TSE)

Compatibilized PHBV/PBSA 70/30 blends with DCP contents of 0, 0.1 and 0.2 phr were compounded using a lab-scale twin-screw extruder with a screw diameter of 18 mm and a length-to-diameter of 16 L/D (SCAMEX, France). The pellets of both polymers and DCP were mixed by hand and introduced in the hopper. The twin-screw extruder temperature zones were set to $175/185/155\text{ }^{\circ}\text{C}$ from the hopper to the die, and the screw speed was 20 rpm. Strands were air-dried and granulated by hand.

2.2.3. Film blowing extrusion

Film blowing was performed with compatibilized PHBV/PBSA 70/30 blends with varying amounts of DCP using a single-screw extruder with a diameter of 20 mm and a L/D ratio of 11 equipped with a small lab-scale film blowing module (SCAMEX, France). The input of the pellets from the TSE was done by hand. The temperature profile was set to $165/170/170/160\text{ }^{\circ}\text{C}$ from hopper to die, and screw speed was maintained at 50 rpm. The film-blowing parameters are summarized in Table 1.

The Blow Up Ratio (BUR) and Draw Down Ratio (DDR) were calculated using the following equations:

$$\text{Blow Up Ratio (BUR)} = \frac{R}{R_o} \quad (1)$$

$$\text{Draw down ratio (DDR)} = (\text{Die gap}/\text{Film thickness})/\text{BUR}, \quad (2)$$

where R and R_o are the bubble and die radius, respectively.

The parameters in Table 1 correspond to the maximum BUR achieved by manually regulating the air pressure of the blowing equipment. The bubble height was approximately 30 cm. After the stable condition was achieved, the process was run approximately 15 min to produce film for characterization. A photo of the equipment and films of the film blowing process are provided in the supplementary information.

Table 1
Film blowing parameters.

	PHBV/PBSA 70/30	PHBV/PBSA 70/30 + 0.1 phr DCP	PHBV/PBSA 70/30 + 0.2 phr DCP
Die diameter	19 mm		
Die gap	1 mm		
Film thickness	$95 \pm 9\ \mu\text{m}$	$122 \pm 30\ \mu\text{m}$	$221 \pm 36\ \mu\text{m}$
Blow up Ratio (BUR)	1.7	2.6	1.3
Draw down ratio (DDR)	6.2 ^a	3.2 ^a	3.5 ^a

^a Based on the average value of the film thickness.

2.3. Characterization of blends and films

2.3.1. Gel content

The compatibilized PHBV/PBSA 70/30 blends with DCP contents of 0, 0.02, 0.1, 0.2, and 1.0 phr were ground into fine powders using a ball mill under liquid nitrogen (Model Retsch MM400, Germany). Two successive Soxhlet extractions were performed to separate PHBV and PBSA. The Soxhlet filters and the samples were dried and weighted. PBSA was dissolved in THF under reflux for approximately 4 h. THF does not dissolve PHBV. After the extraction of PBSA, the remaining PHBV in the Soxhlet filter was dissolved using CHCl_3 under reflux overnight (approximately 18 h). The Soxhlet filter containing the insoluble polymer gel was dried and weighted. The gel fraction was calculated as follows:

$$\text{gel wt. \%} = \frac{m_1}{m_0} \cdot 100\% \quad (4)$$

where m_0 is the original weight of samples and m_1 is the weight of dry residues obtained after dissolution.

2.3.2. Molar mass averages by size-exclusion chromatography

Size-exclusion chromatography (SEC) was performed using a Gilson pump (France) coupled to a Waters autosampler and refractometric index detector (Waters, France). The separation was carried out on a system consisting of a guard column (PLGel 5 μm) and three columns (two columns PLGel 5 μm MIXED-C and one column PLGel 3 μm MIXED E, Agilent Technologies) maintained at 40 $^\circ\text{C}$ in a column oven (Waters, France). The flow rate of the solvents THF (for PBSA) and CHCl_3 (for PHBV) was 1 mL/min. The calibration curve was established for each solvent using three standard kits (EasiVials, 2 mL) containing each four narrow polystyrene standards of molecular weight between $4.69 \cdot 10^3$ and $5.68 \cdot 10^6$ g/mol (Agilent Technologies). Data treatment was done using Empower 3 software (Waters). The sample preparation involved grinding the blends under liquid nitrogen and dissolving PBSA in THF (approximately 10 mg/mL) at room temperature without stirring for 2 h followed by dissolving PHBV in CHCl_3 . The supernatant was sampled after sedimentation of the insoluble phase and filtered before analysis with the help of 0.45 μm Teflon syringe filters using the appropriate solvent as eluent. The final dissolution PHBV is critical and was performed in boiling CHCl_3 (approximately 10 mg/mL) for 12 h.

2.3.3. Rheological properties

The melt flow index (MFI) of the PHBV/PBSA blends was measured according to the ISO 1133 standard procedure using a MFI 4106 device (Zwick, Germany). The samples were extruded through the die under a constant load of 2.16 kg at 190 $^\circ\text{C}$, and the MFI was expressed as the mass passing through the die during a period of 10 min (g/10min).

Dynamic rheology measurements in the melt were performed with a stress-controlled rheometer (MCR 302, Anton Paar, Graz, Austria) using a disk-shaped specimen at 185 $^\circ\text{C}$. The parallel-plate geometry had a gap set between 750 and 800 μm . Dynamic frequency sweep experiments were performed from 0.01 to 100 Hz in the linear visco-elastic region.

2.3.4. Scanning electron microscopy

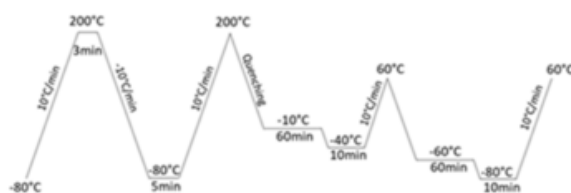
The morphology of the PHBV/PBSA blends was analyzed using Environmental Scanning Electronic Microscopy (ESEM) technology on a FEI Quanta 200 instrument, with an accelerated voltage of 12 kV. To prepare the samples for imaging, they were cryo-fractured using liquid nitrogen and the PBSA phase was selectively dissolved by THF at room temperature for at least 1 h to enhance contrast. The samples were sputter-coated with a thin gold layer using an Emitech K550 Sputter coater. Images were acquired at the cryo-fracture edge of the sample.

2.3.5. Thermal characterization

The thermal properties of the PHBV/PBSA blends were characterized by Differential Scanning Calorimetry (DSC) on a DSC1 instrument from Mettler Toledo (Switzerland). All measurements were conducted under a nitrogen atmosphere (flow rate 50 mL/min) using 5–10 mg of material sealed in 40 μL Aluminum pans. The instrument was calibrated using Indium and Zinc standards. All measurements were duplicated.

The temperature program is shown in Fig. 1. The first cooling and second heating scans (Program I) were to measure the melting and crystallization enthalpies. The glass transition temperature (T_g) of PHBV was measured at the third heating scan after being physically aged at -10 $^\circ\text{C}$, while the T_g of PBSA was measured on the fourth heating scan after being physically aged at -40 $^\circ\text{C}$. Program II (see Fig. 1) was used to analyze the non-isothermal crystallization of PHBV and PBSA. Samples were heated to 190 $^\circ\text{C}$ at a rate of 10 $^\circ\text{C}/\text{min}$, annealed for 3 min to erase any thermal history, and cooled down to -60 $^\circ\text{C}$. Crystallization temperatures (T_c) and exotherms (ΔH_c) were measured at cooling rates of -5 , -10 , -20 , -30 , -40 , and -50 $^\circ\text{C}/\text{min}$. The Pro-

Program I: Determination T_m , T_c and T_g



Program II: Non-isothermal crystallization kinetic

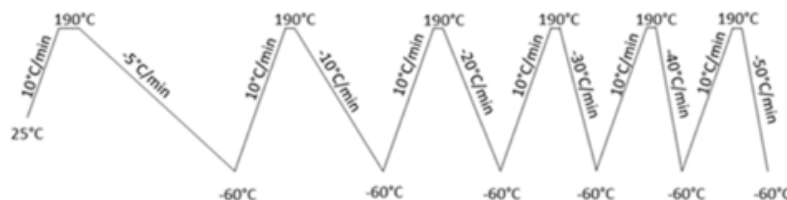


Fig. 1. Differential scanning calorimetry measurement protocol of thermal properties. Protocol II used a sample for -5 , -10 , -20 $^\circ\text{C}/\text{min}$ and a second for -30 , -40 , -50 $^\circ\text{C}/\text{min}$.

gram II was performed on two different samples to decrease the heat treatment of the PHBV. One sample was used for 5, -10, -20 °C and a new one for -30, -40, and -50 °C/min.

The crystallinity of each polymer $\{\chi_i\}_{i=PHBV,PBSA}$ was determined from the endotherm $\Delta H_{m,i}$ as:

$$\chi_i = \frac{\Delta H_{m,i} - \Delta H_{cc,i}}{w_i \Delta H_{m,i}^0} \quad (3)$$

Where w_i is the weight percentage (wt%) of the corresponding polymer, $\Delta H_{cc,i}$ the cold crystallization enthalpy and $\Delta H_{m,i}^0$ the melting enthalpy of a 100% crystalline material with pure PHBV (146 J/g, [27]) and PBSA (113.4 J/g, [28]).

The thermal degradation under N₂ atmosphere was measured using a thermogravimetric analyzer (TGA, Q500, TA Instruments, France). The results are presented in the supporting information.

2.3.6. Mechanical properties

The mechanical properties of the PHBV/PBSA blends were evaluated by tensile and impact testing. To eliminate thickness inhomogeneities, compression-molded specimens were used in the tests. The compression molding process was carried out in a thermal press (SCAMEX 15T, France), where pellets were pre-melted for 3 min and subjected to 80 bars for 1 min, then 150 bars for 1 min. Aluminum foils of 200 μm were used to control the thickness of the samples. Dumbbell-shaped samples of type 5 with a target thickness of 200 μm were cut from the compression-molded sheets. The sample thickness was set from the average of five measurements measured with a caliper.

Tensile tests were conducted under ambient and freezer (-20 °C) temperature. At ambient temperature, tensile properties were measured using a texture analyzer (model TAHD, Stable Micro Systems, UK) equipped with pneumatic grips and with a 5 mm/min crosshead speed. At freezer temperature (-20 °C), tensile tests were performed on a Zwick Z010 instrument (Zwick, Ulm, Germany) with the same crosshead speed.

Unnotched Charpy impact tests were performed according to the ISO 179 standard test method using a Zwick B5113.300 impact tester. Pendulums of 1 and 4 J were used for PHBV-based blends and PBSA, respectively.

A minimum of five samples were tested for each mechanical test and blend formulation.

2.3.7. Physical aging of films in contact with food at -20 °C

Physical aging was conducted on PHBV-based bags upon various storage times at -20 °C and containing parfried frozen French fries (product reference "frites Tradition", McCain, France). The bags were created using blown extrusion film that was cut to a length of 13 cm and thermo-sealed manually on one side using a vacuum packing machine (Model C200, Multivac, Germany) with a sealing time of 0.8 s. The bags were then filled with 25 g of parfried frozen French fries and sealed on the other side. The samples were stored in a freezer at -20 °C for specified periods of time. Before undergoing tensile testing, the sachets were taken out and cut open to discard the food, then the test specimens were cut out of the opened sachets. They were conditioned at 25 °C and 50% RH for a minimum of 24 h. Tensile tests were carried out using a Zwick Z010 instrument with a crosshead speed of 5 mm/min.

3. Results and discussion

3.1. Impact of DCP concentration on melt properties of PHBV/PBSA blends

Fig. 2 shows the variation in torque measured in the mixing chamber during the melt-blending of PHBV with PBSA in a fixed ratio of 70/30 with increasing amounts of DCP. The torque increased with increasing quantity of DCP, which can be attributed to the crosslinking

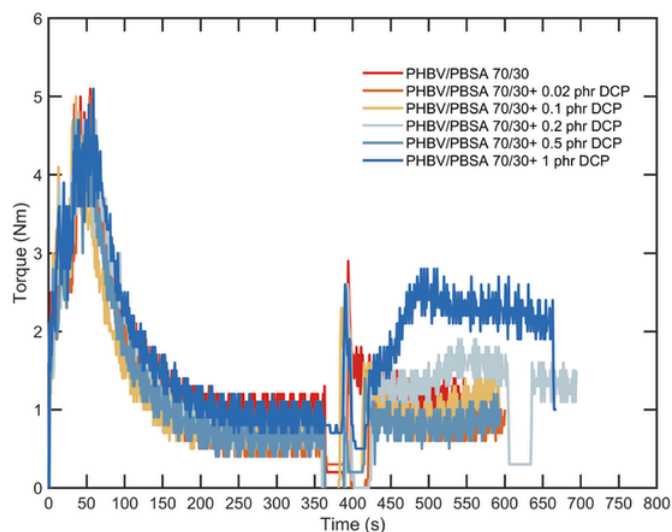


Fig. 2. Measurement of torque over time during melt mixing of compatibilized PHBV/PBSA blends at constant weight ratio 70/30 with different contents of dicumyl peroxide (DCP). The PBSA/DCP dry blend was introduced after 6 min (360 s).

reaction between PHBV and PBSA or crosslinking within a single polymer phase. The gel content, measured to evidence crosslinking, as proposed by Ref. [15], increased with increasing DCP content up to 0.2 phr DCP (see Table 2 and Table 3). However, at 1 phr DCP, it decreased, which may be caused by degradation due to a higher processing temperature at the end of the mixing process. Although regulated, the temperature measured in the mixing chamber for the 0.2 phr blend was 193 °C, while it was 197 °C when 1 phr DCP was added. The gel content measured using TSE pellets had very high variability, and the dry blend method using hand-mixing resulted in a heterogeneous distribution of the gel within the material. Due to the high torque increase caused by 1 phr DCP, the gel-like aspect of the melt, and the high gel content, TSE pellets for film-blown extrusion were produced using only 0.1 and 0.2 phr DCP.

Table 2

Gel content and molar mass averages of PHBV/PBSA blends with different concentrations of DCP.

Samples	Process	Gel content (%)	PHBV			PBSA		
			M _n	M _w	D	M _n	M _w	D
PHBV ^a	Batch	2 ± 2	n.p.	n.p.	n.p.			
PHBV ref.	Mixer		113,000	290,900	2.6			
PBSA ^a		1 ± 1				140,000	204,600	1.5
Blend 70/30		2 ± 2	36,500	60,200	1.7	21,100	36,700	1.7
+0.02 phr		8 ± 6	31,300	57,200	1.8	6400	11,100	1.7
0.1 phr		9 ± 4	79,800	149,000	1.9	10,200	21,500	2.1
0.2 phr		36 ± 4	n.p.	n.p.	n.p.	9500	25,800	2.7
1 phr		24 ± 2	n.p.	n.p.	n.p.	10,900	24,900	2.2
Blend 70/30	TSE	n.d.	51,600	94,900	1.8	22,700	39,300	1.7
0.1 phr		16 ± 1	n.p.	n.p.	n.p.	23,200	63,300	2.7
0.2 phr		28 ± 12	n.p.	n.p.	n.p.	18,180	35,100	1.9

^a values of initial pellets, n.p. not present, n.d. not determined, empty field = no sample, PHBV molar mass data obtained from Ref. [29].

Table 3

Melt Flow Index and Gel content of PHBV/PBSA with varying content of DCP measured after the different blend fabrication methods.

Samples	Melt Flow Index (g/10min)	
	Batch Mixer	TSE
Neat PHBV ^a	90 ± 3	30 ± 1
Neat PBSA ^a	2.5 ± 0.1	2.5 ± 0.7
70/30	67 ± 2	45 ± 1
0.1 phr	22 ± 1	13 ± 1
0.2phr	21 ± 1	17 ± 1
1 phr	20 ± 1	

^a MFI values of neat pellets, two different batches of PHBV were used, empty field = no sample.

The degradation of macromolecular chains during processing was analyzed using SEC, and the results are presented in Table 2. The PHBV pellets were difficult to dissolve, even after grinding under nitrogen, and therefore the amount of PHBV in solution remained below the detection limit. The molecular mass averages of PHBV from the same supplier were reported in the literature [29,30] and were added to Table 2. The blending process resulted in a substantial loss of the macromolecular weight averages of PHBV, which is a well-known problem due to the low processing stability of PHBV and its tendency to degrade by a back-biting reaction at temperatures close to its melting point [1]. TSE processing caused probably less damage than batch mixing, but still led to a significant decrease in the macromolecular chain length. The increase in the DCP quantity resulted in an increase in the molar mass averages of PHBV, likely due to crosslinking with PBSA and the chain extension of PHBV during mixing. At high DCP and gel contents, the solubility of the PHBV phase was low again, and no PHBV peaks could be detected, which might be explained by preferential crosslinking in the PHBV phase, decreasing its solubility.

Few studies on the chemical degradation of PBSA exist, but the main mechanism is likely thermal hydrolysis, as evidenced in other polyesters [20]. The macromolecular mass averages of PBSA decreased significantly, possibly due to the insufficient drying procedure of the PBSA pellets. The use of DCP did not change the degradation behavior, which reinforces the hypothesis that the crosslinking reaction preferentially takes place in the PHBV phase.

3.2. Rheological properties of compatibilized PHBV/PBSA blends

The impact of the DCP-induced crosslinking reaction on the melt strength and melt viscosity was evaluated. The results for MFI are presented in Table 3. The MFI values of the initial pellets were very different. They correspond to two different batches of PHBV purchased from the same supplier. PHBV had in any case much higher MFI than PBSA. The PHBV/PBSA (70/30) blend had an intermediate value. As already observed in Table 2, the mixing caused damage in the chain length of PHBV and increased the MFI value in the case of TSE. Interestingly, DCP helped to stabilize the MFI value, even if the initial PHBV quality was low. The addition of 0.1 phr DCP decreased the MFI from 67 to 22 g/10min, while further increases in DCP had no effect. Samples produced through TSE before film blowing had lower MFI compared to those produced through batch mixing due to lower thermal degradation and better initial quality. In addition to thermal degradation, a coarser emulsion obtained by batch mixing could also decrease viscosity because of less interfacial stress.

The complex viscosity (η^*) of non-compatibilized and compatibilized PHBV blends produced by batch mixing is shown in Fig. 3a. The rheological properties of blends produced by TSE were similar. The experimental curves can be found in the supporting information S4. At DCP concentrations below 0.1 phr, no significant change in η^* was observed. At DCP concentrations above 0.1 phr, η^* increased by two magnitude orders at low frequencies. Shear-thinning was observed at

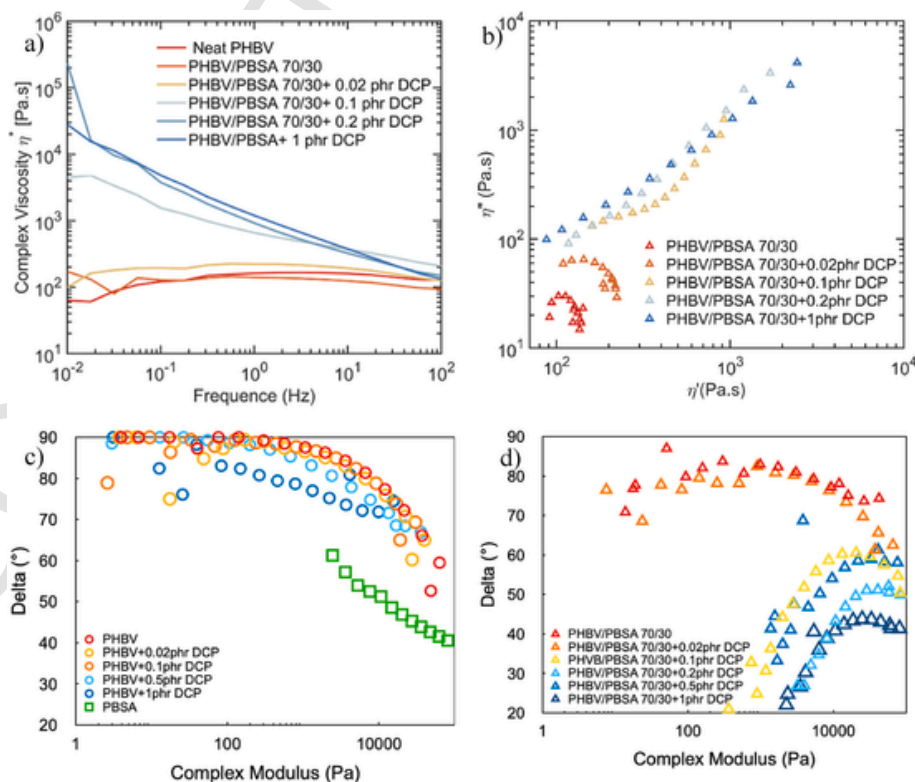


Fig. 3. Rheological properties of PHBV/PBSA 70/30 blends. (a) Complex viscosity η^* of blends obtained by batch mixing at 185 °C as function of frequency; (b) Cole-Cole plots of PHBV/PBSA 70/30 compatibilized with DCP using different concentrations (0.02–1 phr); (c) van Gurp-Palmen plot of PHBV mixed with DCP and PBSA; (d) van Gurp-Palmen plot of blends compatibilized with DCP.

high frequencies, which is a characteristic of polymer systems with long chain branched structures [31]. The curve showed an increase at low frequencies, which may indicate a very high zero shear viscosity resulting from the gel content.

The Cole-Cole plots, which plot the out-of-phase component (η'') versus the in-phase component of the complex viscosity (η') are depicted in Fig. 3b. These plots are highly sensitive to the phase structures in polymer blends [32]. When the DCP concentration was low (0.02 phr), both the compatibilized and non-compatibilized PHBV/PBSA blends showed a semicircular shape, indicating that the structural relaxation of PHBV and PBSA could not be discriminated. However, when the DCP concentration exceeded the threshold value of 0.1 phr, the Cole-Cole plots deviated from a circular shape evolved almost linearly in log-log scale. This indicates that the chain relaxation became hindered, which would be characteristic of branching or crosslinking [32]. The changes in the viscoelastic behavior of the samples can be observed thanks to the mechanical spectra shown in the supporting information. Chain branching indicated by the Cole-Cole plot was also observed in compatibilized PLA/PBSA blends [33]. The Cole-Cole plot alone is however not indicative enough, especially long chain branching is not easy to be observed. The van Gurp-Palmen plot, which shows the phase angle as a function of the complex modulus, can be used to classify specific macromolecular architectures [34]. It is presented in Fig. 3c and d for PHBV and PHBV/PBSA blends. Because of the degradation of PHBV it was difficult to obtain stable values of the shear moduli in the plateau region. Therefore, we present the non-reduced plot. PHBV and PBSA show the signature of linear polymer chains [34]. The curve changed to smaller angle values when more than 0.5 phr DCP was added to PHBV (Fig. 3c). A bump at high modulus (high frequency) appeared in the PHBV/PBSA blends when more than 0.02 phr DCP were added (Fig. 3d). This pattern is characteristic of a mixture of linear macromolecules and macromolecules with long-chain branching [34]. To conclude, the increase in DCP concentration resulted most probably in the formation of crosslinked structures, evidenced by the gel content, and long-chain branched structures, evidenced by the van Gurp-Palmen plot. In particular long-chain branching increases the melt viscosity. A positive effect on processing using film blow extrusion would be expected.

3.3. Morphology of compatibilized PHBV/PBSA blends

The morphologies resulting from melt blending of PHBV/PBSA 70/30 in the presence of DCP were observed by SEM and are presented in Fig. 4a–d. Without the addition of DCP, large PBSA droplets were dispersed within the PHBV matrix (Fig. 4a). At a DCP concentration of 0.02 phr DCP, the diameter of PBSA droplet decreased from very large droplets with a radius up to 25 μm to a radius of approximately 50% of droplets below 3.8 μm , but with a wide range of sizes (Fig. 4b). The histogram of the size distribution corresponding to Fig. 4b is shown in the supporting information. At higher DCP concentrations, the SEM resolution was not sufficient to distinguish nodules (Fig. 4c and d). This reduction in domain size can be attributed to the compatibilization of PHBV and PBSA either through crosslinking at the interface, the preferential chain extension of PHBV (Table 2), or to the reduction of the interfacial tension between the two polymers due to the formation of PHBV-g-PBSA molecules.

3.4. Thermal properties of PHBV/PBSA blends

The thermal properties of the PHBV/PBSA blends are summarized in Table 4. The blending process led to a slight decrease of the glass transition temperature (T_g) of PHBV and PBSA, which can mostly be attributed to the decrease in the molecular mass averages (as shown in Table 2). The concentration of DCP in the blends and the processing method had no significant impact on the T_g of either PHBV or PBSA. Both polymer are immiscible [8] and some crosslinking between both phases (interpretation of Fig. 3) did not change their overall glass transition. The melting temperatures (T_m) of both polymers in the blends were lower than that of their neat counterparts. The T_m of both polymers decreased further at the highest concentration of DCP. The non-isothermal crystallization peak of PHBV in the blends shifted to lower temperatures, while the one of PBSA to higher temperatures, as already discussed in our earlier study [8]. The crystallinity degree of both polymers decreased with increasing DCP content.

To gain insights on the changes in the crystallinity with temperature, a kinetic study of the non-isothermal crystallization was performed using the Avrami [35–37]-Jeziorny [38] method and inter-

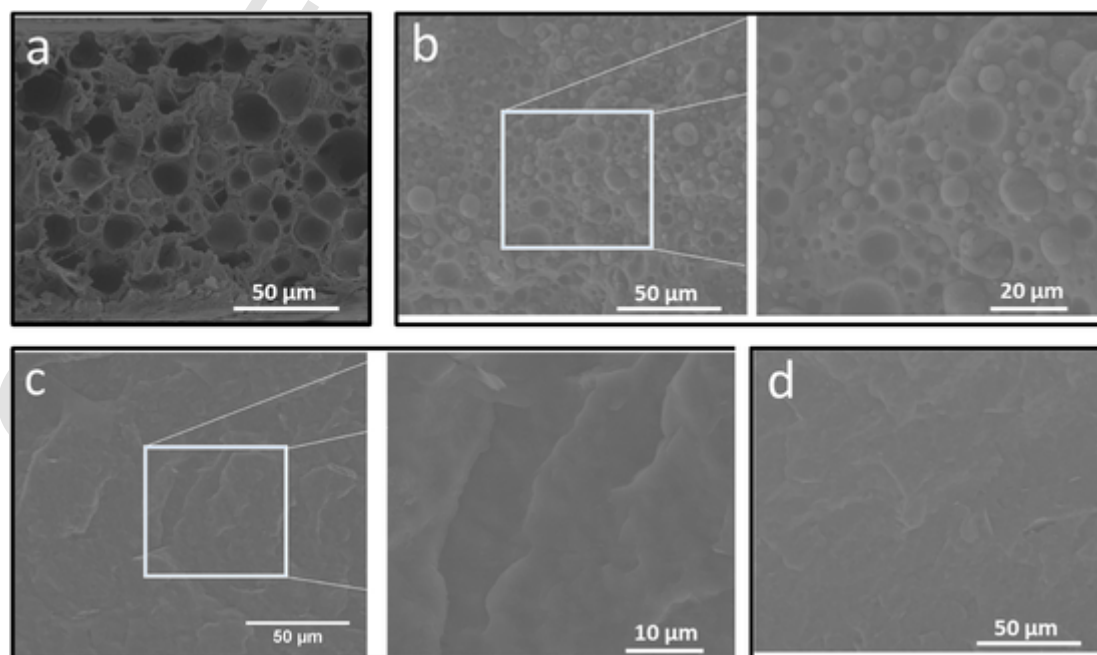


Fig. 4. SEM images of cryo-fractured surfaces of compatibilized PHBV/PBSA blends fabricated with different DCP contents using the batch mixer: (a) 0 phr, (b) 0.02 phr at two magnifications, (c) 0.1 phr at two magnifications, and (d) 0.2 phr.

Table 4

Thermal properties of neat PHBV, PBSA, PHBV/PBSA 70/30, and compatibilized PHBV/PBSA blends with different content of DCP evaluated by DSC at the second heating scan. The T_g was analyzed using the aging method (see Fig. 1).

Samples		T_m (°C)		T_c (°C)		χ (%)		Glass transition temperature (T_g)	
		PHBV	PBSA	PHBV	PBSA	PHBV	PBSA	PHBV	PBSA
Batch Mixer	Neat PHBV	171 ± 3		122 ± 1		68 ± 1		2.4 ± 0.4	
	Neat PBSA		88 ± 3		38 ± 3		45 ± 4	-45.9 ± 1.6	
	70/30	169 ± 2	86 ± 2	117 ± 1	50 ± 1	67 ± 2	33 ± 5	-1.5 ± 0.1	-48.6 ± 2
	0.02 phr	169 ± 1	85 ± 1	118 ± 1	53 ± 4	66 ± 0	28 ± 0	-1.3 ± 0.1	-49.6 ± 0.5
	0.1 phr	169 ± 1	85 ± 1	117 ± 1	54 ± 1	63 ± 2	29 ± 5	-1.1 ± 0.7	-48.9 ± 1.3
	0.2phr	168 ± 1	83 ± 1	118 ± 1	54 ± 1	67 ± 2	22 ± 9	-1.3 ± 1.1	-48.7 ± 0.9
	1 phr	163 ± 1	75 ± 1	118 ± 1	51 ± 1	64 ± 0	21 ± 1	-2.0 ± 1.6	-48.1 ± 1.3
TSE	70/30	170 ± 1	86 ± 1	119 ± 1	56 ± 1	72 ± 7	32 ± 1	-1.1 ± 0.7	-49.6 ± 0.5
	0.1 phr	169 ± 1	80 ± 1	117 ± 1	57 ± 1	64 ± 1	32 ± 1	-0.9 ± 0.4	-48.1 ± 0.2
	0.2 phr	169 ± 1	83 ± 1	118 ± 1	56 ± 1	69 ± 1	24 ± 3	-0.5 ± 0.2	-48.7 ± 0.7

interpreted according to the Liu and Mo's model [39]. The equations and the raw data are available in the supporting information. Fig. 5a reports the half-time of crystallization ($t_{1/2}$) at a given cooling rate, which was calculated from the Avrami-Jeziorny constants (Fig. 5a and b). The analysis shows that the crystallization kinetics of PHBV at low cooling rates were slightly faster in the blends compared to neat PHBV, but no significant impact of DCP on the kinetics was observed (Fig. 5a). This small decrease in $t_{1/2}$ was attributed to the nucleation of PHBV by PBSA. Because all samples were subjected to the same heating program, we neglected in the analysis an eventual impact of thermal degradation. As reported in our earlier study, the crystallization rate of PBSA in the blends was clearly increased because neat PBSA could not crystallize at cooling rates higher than 10 °C/min [8]. The accelerated crystallization of PBSA was likely due to nucleation. DCP seemed to speed up the non-isothermal crystallization of PBSA, but no impact of concentration was found (Fig. 5b). The parameter $F(T)$ of the Liu and Mo model, which represents the required cooling rate to obtain a given crystallinity degree, is shown as a function of crystallinity degree in Fig. 5c and d. The higher $F(T)$, the more difficult the crystallization becomes. $F(T)$ in-

creased for both PHBV and PBSA, indicating an increasing hindrance of the crystallization process at high crystallinity degrees. However, the blend structure seemed to facilitate the crystallization process of PHBV, as $F(T)$ of the blends was lower than that of neat PBSA, which corresponds to our earlier observations [8]. No clear impact of the presence of DCP was observed. In conclusion, DCP was an effective compatibilizing agent between PHBV and PBSA; it had no significant impact on the crystallization behavior of both phases in the blend.

3.5. Mechanical properties

The mechanical properties of the blends were evaluated through tensile testing, and the results are presented in Table 5. Typical stress/strain curves are shown in the supporting information. Despite their brittle behavior, all blends showed a slightly higher elongation at break compared to neat PHBV. The brittleness of PHBV with low 3HV contents is well-known and it is caused by the cold crystallization of the residual amorphous phase at ambient temperature, as well as radial or circumferential cracks that can form inside spherulites of PHBV

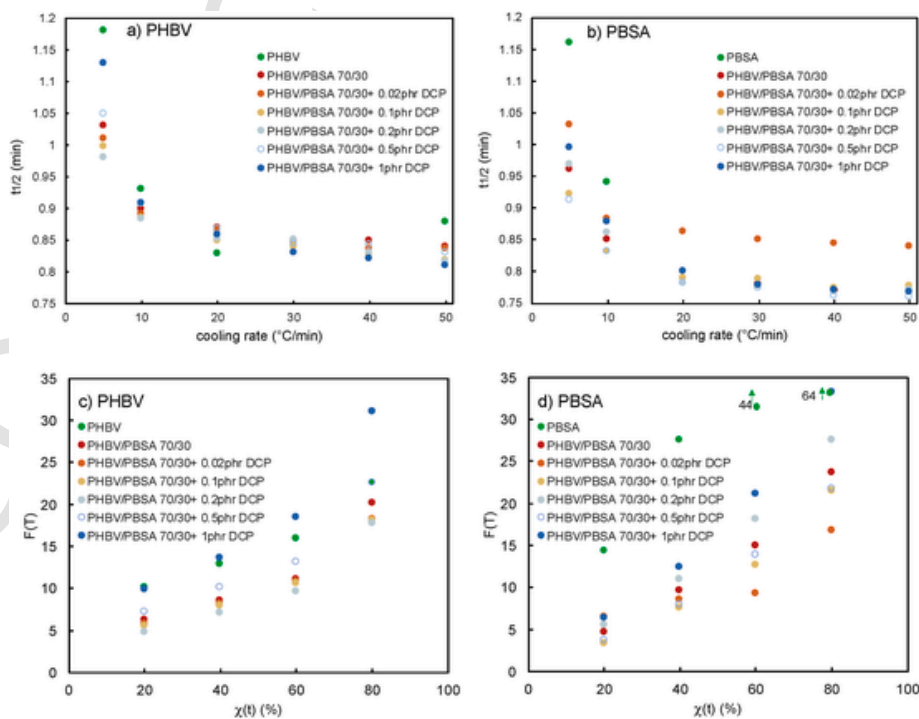


Fig. 5. Kinetic parameters of non-isothermal crystallization from the melt of PHBV and PBSA in compatibilized blends. The half-time of crystallization ($t_{1/2}$) (figures a and b) was obtained from the Avrami-Jeziorny parameters. The difficulty to reach a specific crystallinity degree (χ_c) was estimated by the $F(T)$ parameter, calculated using the Liu and Mo model (figures c and d). The values of neat PHBV and PBSA were taken from our earlier work [8].

Table 5

Mechanical properties of PHBV/PBSA blends with varying content of DCP obtained by tensile testing at 23 °C.

Sample	Young modulus (MPa)	Maximum stress (MPa)	Elongation at break (%)	Impact Strength (kJ.m ⁻²)
Batch Mixer				
Neat PHBV	3485 ± 60	22 ± 2	0.98 ± 0.1	2.0 ± 0.6
Neat PBSA	332 ± 8	15 ± 1.4	134.8 ± 48	32.4 ± 4.1
70/30	2227 ± 110	19 ± 2	1.5 ± 0.4	n.d
0.02 phr	2222 ± 100	20 ± 2	1.4 ± 0.2	
0.1 phr	1973 ± 120	21 ± 3	1.9 ± 0.2	
0.2 phr	1879 ± 230	19 ± 6	1.9 ± 0.5	
1 phr	1742 ± 300	13 ± 3	1 ± 0.1	
TSE ^a 70/30	1807 ± 80	15 ± 3	1.6 ± 1.4	n.d
0.1 phr	1703 ± 140	17 ± 4	2.0 ± 0.5	2.8 ± 0.3
0.2 phr	1713 ± 80	17 ± 2	2.1 ± 0.4	6.8 ± 0.2

^a Samples were thermo-compression molded, n.d. not determined.

[40,41]. As previously reported [8], the melt mixing of PHBV with PBSA did not improve the elongation at break. In detail, the stress at break decreased even compared to PHBV due to ruptures at the PHBV/PBSA interface. The maximum stress of the compatibilized PHBV/PBSA blends at 0.02, and 0.1 phr was almost equal to PHBV, which can be attributed to successful compatibilization. However, at DCP concentrations greater than 0.1 phr, the maximum stress decreased, which might be caused by the higher gel fraction acting as defects and leading to fracture.

The fracture surfaces of the PHBV/PBSA blends were observed in SEM and are presented in Fig. 6. The SEM images showed neat fracture surfaces in the blends. At DCP concentrations greater than 0.02 phr, the formation of small stretched fibers due to matrix yielding was detected in some locations (Fig. 6c and d). This type of morphology has already been reported for compatibilized PLA/PBAT blends in the presence of DCP [13]. At DCP concentration of 1 phr, a denser structure with fewer elongated fibrils was observed (Fig. 6e), which was consistent with the decrease of the elongation at break as reported in Table 5.

The Charpy impact strength of the TSA samples was evaluated and is presented in Table 5. The impact strength increased with increasing DCP content. At a DCP concentration of 0.2 phr, it was roughly three times higher than the impact strength of PHBV, indicating that PBSA contributes to energy dissipation inside the material. In conclusion, while there were some changes in the fracture of compatibilized PHBV/PBSA blends, they were not sufficient to overcome the inherent brittleness of the PHBV crystals.

3.6. Film-blowing of compatibilized PHBV/PBSA blends

Fig. 7 demonstrates the ability of the PHBV/PBSA blend containing 0, 0.1 and 0.2 phr DCP to be processed by film blowing. The bubble of the non-compatibilized PHBV/PBSA blend was difficult to stabilize and showed some draw resonance. The films were very thick because of the small blow-up ratio (BUR). The addition of 0.1 phr DCP improved the melt strength and added extensional viscosity, resulting in greater film-blowing stability, as evidenced by the greater BUR reported in Table 1. With the increase of the BUR, the draw down ratio (DDR) was decreased, which can have an additional positive effect on bubble stability. However, there was still some draw resonance. A short movie of the process is provided in the supplementary information. However, films containing 0.2 phr DCP showed white aggregates (as seen in the inset of Fig. 7) and reduced extensibility. This was due to the high gel content,

which was found to act as defect points and prevent blends from being blown properly.

In conclusion, the compatibilization was beneficial for the processability (higher BUR, lower DDR) of the PHBV/PBSA blends due to the significant decrease in the melt flow index and increase in melt viscosity. This allowed for the successful film blowing of PHBV/PBSA blends compatibilized with 0.1 phr DCP, where PHBV was the major component.

3.7. Aging of PHBV/PBSA blends in food contact under frozen conditions

Frozen foods represent a significant market for flexible food packaging films, as they require portioning and protection during long-term storage. The films must perform across a wide temperature range and for extended periods of time. The tensile properties of blends produced by TSE and thermocompression were evaluated at freezer temperature (−20 °C) and are compared to the properties at ambient temperature in Table 6. As expected, the elastic modulus and ultimate strength increased, and the elongation at break decreased at −20 °C due to PHBV being in its glassy state.

The films were capable of being hot-sealed, which allowed the creation of plastic bags filled with frozen fatty food (Fig. 8a). Parfried frozen French fries were targeted as food products because they combined several challenges, including the simultaneous presence of moisture and oil. The bags were stored at −20 °C, and no evidence of delamination at the sealing line was observed over time.

The evolution of the elastic modulus and the elongation at break over time is shown in Fig. 8b and c and remained essentially stable. Previously, the aging of PHBV was only studied at ambient temperature, where the mechanical properties of PHBV stabilized after 15 days of aging [27,42], mainly due to secondary crystallization [43]. At freezing temperatures, PHBV can become brittle due to physical aging, but no changes were detected in this study. In conclusion, the extrusion-blown films of compatibilized PHBV/PBSA blends can be used for the packaging of frozen food.

4. Conclusions

This study aimed to develop PHBV blends that could be processed by film-blowing extrusion with a majority of PHBV content. Building on our previous work, a blend composition of 70 wt% PHBV and 30 wt% PBSA was used, with DCP serving as the reactive compatibilizer. The processing of PHBV and PBSA blends with DCP in melts resulted in compatibilized blends with significantly decreased melt flow index and increased melt viscosity. The measurement of the gel content showed that crosslinking reactions occurred primarily in the PHBV phase, and Cole-Cole and van Gurp-Palmen plots indicated a transformation of macromolecules from linear to long-chain branched structures. The formulation with a high viscosity polymer and the structural changes enabled the successful film-blown extrusion of the blends.

The mechanical properties of the blends showed a lower elastic modulus and yield strength of the films, but they still displayed brittle behavior. Using a ductile secondary polymer and compatibilization alone was not sufficient to overcome the inherent brittleness of PHBV. However, the impact strength was improved by three times. A long-term storage experiment of frozen food (French fries) in heat-sealed PHBV/PBSA films demonstrated that the mechanical properties of the blown films were stable for 6 months under freezer conditions (−20 °C).

In conclusion, even though the blown films of formulated PHBV are still brittle, they have the potential to become a performing packaging material for food. A more detailed work on the processing parameters will yet be needed to better characterize the processing window of these formulations.

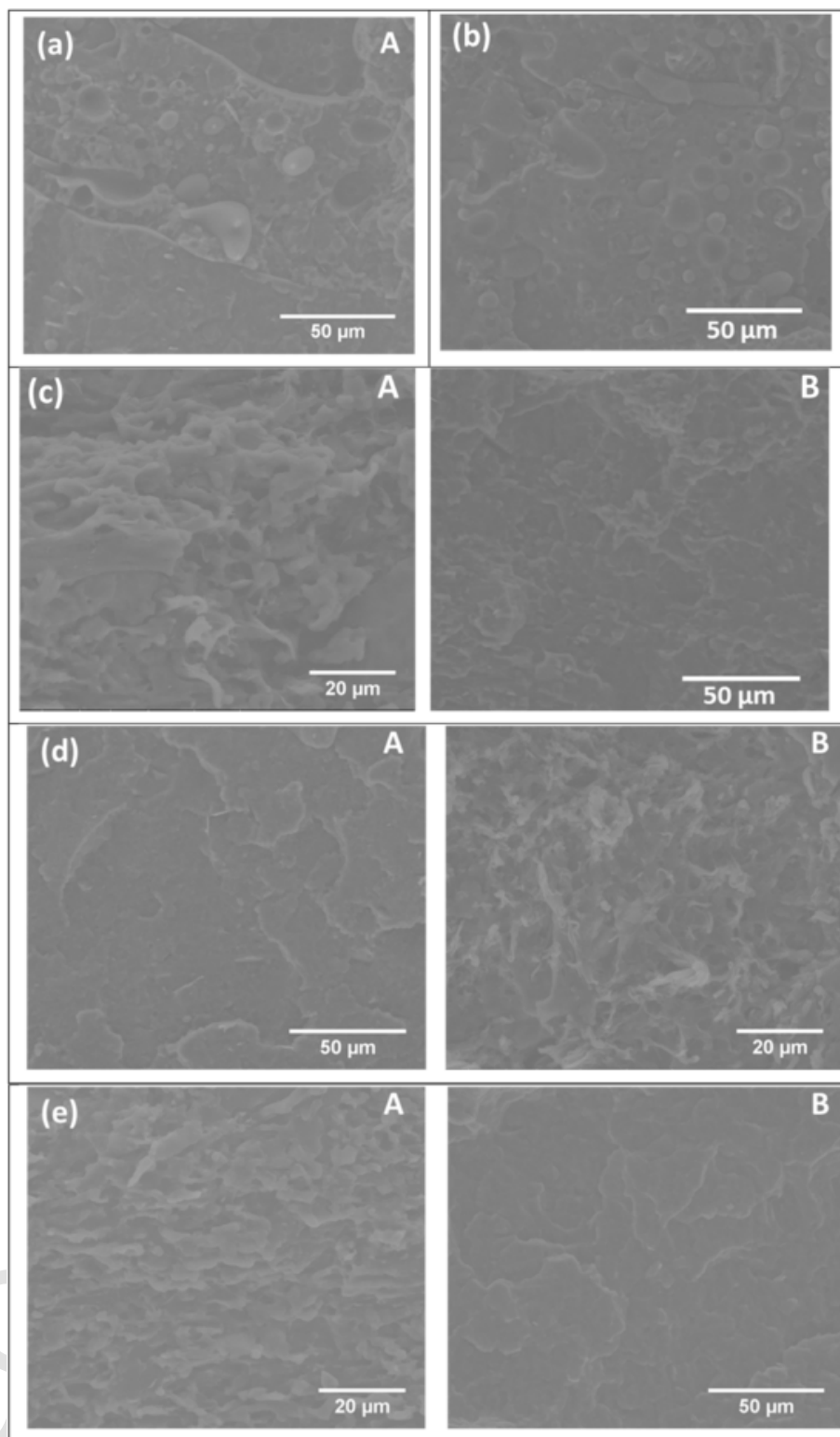


Fig. 6. SEM images of the fracture surface of compatibilized PHBV/PBSA blends with different DCP content at different localizations (marked as A and B): a) 0 phr, b) 0.02 phr, c) 0.1 phr, d) 0.2 phr, and e) 1 phr.

Credit author statement

Benjamin Le Delliou: Conceptualization, Investigation, Methodology, Writing - Original Draft, Polymer blends, formulation, batch mixing, extrusion, physical analysis (morphology, rheology, calorimetry, applicative tests).

Olivier Vitrac: Conceptualization, Investigation, Methodology, Writing - Original Draft, Review & Editing, Polymer blends and analysis, Food Contact Materials.

Anir Benihya: Investigation, Methodology, Polymer analysis – chemical analyses (blend formulation, SEC, gel point).

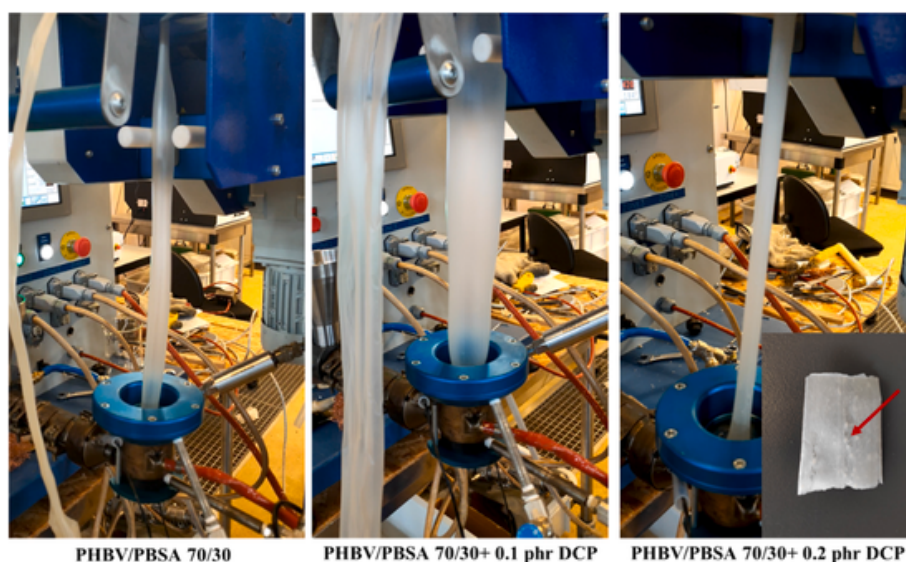


Fig. 7. Film blowing of PHBV/PBSA 70/30 with compatibilization with DCP.

Table 6

Evolution of the elastic modulus, elongation at break, and stress at break of the different melt blown PHBV/PBSA blends compatibilized with DCP with at different temperatures. Typical raw data are shown the supporting information.

Sample	+20 °C			−20 °C		
	Young modulus (MPa)	Maximum stress (MPa)	Elongation at break (%)	Young modulus (MPa)	Maximum stress (MPa)	Elongation at break (%)
Neat PHBV ^a	3485 ± 63	22 ± 2	1 ± 0.2	5691	35 ± 12	0.8 ± 0.2
Neat PBSA ^a	332 ± 8	15 ± 1	135 ± 48	395	29 ± 6	39 ± 17
70/30	1807 ± 80	15 ± 3	1.6 ± 0.4	2929	24 ± 10	0.9 ± 0.2
0.1 phr	1703 ± 140	17 ± 4	2.0 ± 0.5	3374	29 ± 6	1.6 ± 0.2
0.2phr	1714 ± 80	17 ± 2	2.1 ± 0.4	3003	34 ± 6	1.5 ± 0.3

^a Values of the neat polymers evaluated after thermocompression of the pellets repeated from Table 5.

Patrice Dole: Conceptualization, Investigation, Methodology, Writing - Original Draft, Polymer processing, twin screw extrusion, film blowing, Food Contact Materials.

Sandra Domenek: Conceptualization, Investigation, Project administration, Writing - Original Draft, Review & Editing, Polymer blending, formulation, physical and chemical analysis, Food Contact Materials.

Note on funding. The authors acknowledge financial support from the company McCain Alimentaire S.A.S and from ANRT (French National Association for Research and Technology) via the CIFRE agreement n°2017/1574 attributed to Benjamin Le Delliou.

Declaration of competing interest

The authors declare that they have no known competing financial interests or personal relationships that could have appeared to influence the work reported in this paper.

Data availability

Data will be made available on request.

Acknowledgments

The authors acknowledge financial support from the company McCain Alimentaire S.A.S and from ANRT (French National Association for Research and Technology) via the CIFRE agreement n°2017/1574 attributed to Benjamin Le Delliou. The authors greatly thank Dr. Pierre Gondé for his technical support. Furthermore, we thank Dr. Florian Pion (UMR IJPB, AgroParisTech, INRAE, University Paris Saclay, 78000 Versailles, France) for NMR analysis and Dr. Mickael Castro (University Bretagne Sud, UMR CNRS 6027, IRDL, 56100 Lorient, France) for his support in rheological measurements.

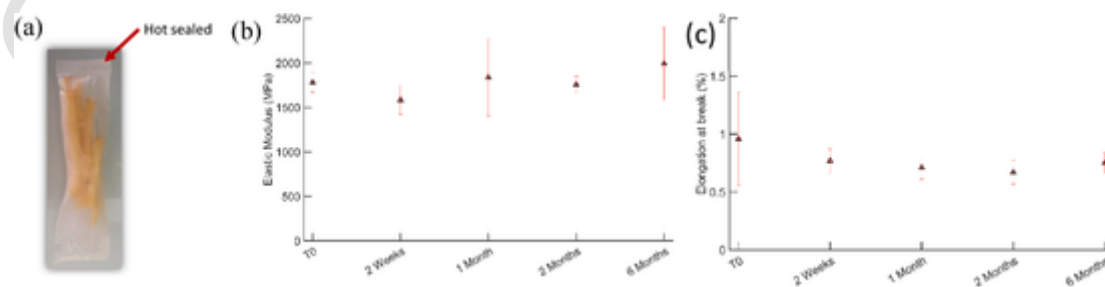


Fig. 8. (a) Hot sealed film of PHBV/PBSA + 0.1phr DCP filled with frozen French fries and evolution of (b) the elastic modulus and (c) the elongation at break of PHBV/PBSA 70/3 + 0.1 phr DCP in contact with frozen French fries during storage at −20 °C.

Appendix A. Supplementary data

Supplementary data to this article can be found online at <https://doi.org/10.1016/j.polymertesting.2023.108072>.

References

- [1] B. Laycock, P. Halley, S. Pratt, A. Werker, P. Lant, The chemomechanical properties of microbial polyhydroxyalkanoates, *Prog. Polym. Sci.* 39 (2014) 397–442.
- [2] M. Deroine, G. Cesar, A. Le Duigou, P. Davies, S. Bruzaud, Natural degradation and biodegradation of poly(3-hydroxybutyrate-co-3-hydroxyvalerate) in liquid and solid marine environments, *J. Polym. Environ.* 23 (2015) 493–505.
- [3] P. Kumar, S. Ray, V.C. Kalia, Production of co-polymers of polyhydroxyalkanoates by regulating the hydrolysis of biowastes, *Bioresour. Technol.* 200 (2016) 413–419.
- [4] A. Elain, A. Le Grand, Y.M. Corre, M. Le Fellic, N. Hachet, V. Le Tilly, P. Loulergue, J.L. Audic, S. Bruzaud, Valorisation of local agro-industrial processing waters as growth media for polyhydroxyalkanoates (PHA) production, *Ind. Crop. Prod.* 80 (2016) 1–5.
- [5] P. Lemechko, M. Le Fellic, S. Bruzaud, Production of poly(3-hydroxybutyrate-co-3-hydroxyvalerate) using agro-industrial effluents with tunable proportion of 3-hydroxyvalerate monomer units, *Int. J. Biol. Macromol.* 128 (2019) 429–434.
- [6] R.A.J. Verlinden, D.J. Hill, M.A. Kenward, C.D. Williams, Z. Piotrowska-Seget, I.K. Radecka, Production of Polyhydroxyalkanoates from Waste Frying Oil by Cupriavidus Necator, *Amb Express*, 2011, p. 1.
- [7] M. Carvalheira, L. Hilliou, C.S.S. Oliveira, E.C. Guarda, M.A.M. Reis, Polyhydroxyalkanoates from industrial cheese whey: production and characterization of polymers with differing hydroxyvalerate content, *Curr. Res. Biotechnol.* 4 (2022) 211–220.
- [8] B. Le Delliou, O. Vitrac, M. Castro, S. Bruzaud, S. Domenek, Characterization of a new bio-based and biodegradable blends of poly(3-hydroxybutyrate-co-3-hydroxyvalerate) and poly(butylene-co-succinate-co-adipate), *J. Appl. Polym. Sci.* 139 (2022) 52124.
- [9] J. Sikora, L. Majewski, A. Puszka, Modern biodegradable plastics—processing and properties: Part I, *Materials* 13 (2020) 1986.
- [10] J.H. Wang, Y.C. Tian, B. Zhou, Degradation and stabilization of poly(butylene adipate-co-terephthalate)/polyhydroxyalkanoate biodegradable mulch films under different aging tests, *J. Polym. Environ.* 30 (2022) 1366–1379.
- [11] M. Cunha, B. Fernandes, J.A. Covas, A.A. Vicente, L. Hilliou, Film blowing of PHBV blends and PHBV-based multilayers for the production of biodegradable packages, *J. Appl. Polym. Sci.* 133 (2016) n/a-n/a.
- [12] P.F. Teixeira, J.A. Covas, M.J. Suarez, I. Angulo, L. Hilliou, Film blowing of PHB-based systems for home compostable food packaging, *Int. Polym. Process.* 35 (2020) 440–447.
- [13] P. Ma, X. Cai, Y. Zhang, S. Wang, W. Dong, M. Chen, P. Lemstra, In-situ compatibilization of poly (lactic acid) and poly (butylene adipate-co-terephthalate) blends by using dicumyl peroxide as a free-radical initiator, *Polym. Degrad. Stabil.* 102 (2014) 145–151.
- [14] A.R. Kolahchi, M. Kontopoulou, Chain extended poly(3-hydroxybutyrate) with improved rheological properties and thermal stability, through reactive modification in the melt state, *Polym. Degrad. Stabil.* 121 (2015) 222–229.
- [15] P. Ma, D.G. Hristova-Bogaerds, P.J. Lemstra, Y. Zhang, S. Wang, Toughening of PHBV/PBS and PHB/PBS blends via in situ compatibilization using dicumyl peroxide as a free-radical grafting initiator, *Macromol. Mater. Eng.* 297 (2012) 402–410.
- [16] M. Cunha, B. Fernandes, J.A. Covas, A.A. Vicente, L. Hilliou, Film blowing of PHBV blends and PHBV-based multilayers for the production of biodegradable packages, *J. Appl. Polym. Sci.* 133 (2016).
- [17] S.L. Sun, P.F. Liu, N. Ji, H.X. Hou, H.Z. Dong, Effects of low polyhydroxyalkanoate content on the properties of films based on modified starch acquired by extrusion blowing, *Food Hydrocolloids* 72 (2017) 81–89.
- [18] P.J. Jandas, S. Mohanty, S.K. Nayak, Sustainability, compostability, and specific microbial activity on agricultural mulch films prepared from poly(lactic acid), *Ind. Eng. Chem. Res.* 52 (2013) 17714–17724.
- [19] M. Cunha, M.A. Berthet, R. Pereira, J.A. Covas, A.A. Vicente, L. Hilliou, Development of polyhydroxyalkanoate/beer spent grain fibers composites for film blowing applications, *Polym. Compos.* 36 (2015) 1859–1865.
- [20] T. Debuissy, E. Pollet, L. Avérous, Synthesis and characterization of biobased poly(butylene succinate-ran-butylene adipate). Analysis of the composition-dependent physicochemical properties, *Eur. Polym. J.* 87 (2017) 84–98.
- [21] V. Ojijo, S. Sinha Ray, R. Sadiku, Toughening of biodegradable polylactide/poly (butylene succinate-co-adipate) blends via in situ reactive compatibilization, *ACS Appl. Mater. Interfaces* 5 (2013) 4266–4276.
- [22] A. Mirzadeh, H. Ghasemi, F. Mahrous, M.R. Kamal, Reactive extrusion effects on rheological and mechanical properties of poly(lactic acid)/poly (butylene succinate)-co-adipate/epoxy chain extender blends and clay nanocomposites, *J. Appl. Polym. Sci.* 132 (2015) 11.
- [23] H. Eslami, M.R. Kamal, Effect of a chain extender on the rheological and mechanical properties of biodegradable poly(lactic acid)/poly[(butylene succinate)-co-adipate] blends, *J. Appl. Polym. Sci.* 129 (2013) 2418–2428.
- [24] D. Lascano, L. Quiles-Carrillo, R. Balart, T. Boronat, N. Montanes, Toughened poly (lactic acid)/PLA formulations by binary blends with poly(butylene succinate-co-adipate)PBSA and their shape memory behaviour, *Materials* 12 (2019) 14.
- [25] S. Coiai, M.L. Di Lorenzo, P. Cinelli, M.C. Righetti, E. Passaglia, Binary Green Blends of Poly(lactic acid) with Poly(butylene adipate-co-butylene terephthalate) and Poly(butylene succinate-co-butylene adipate) and Their Nanocomposites, *Polymers* 13 (2021) 2489.
- [26] B. Mallet, K. Lamnawar, A. Maazouz, Improvement of blown film extrusion of poly(lactic acid): structure–processing–properties relationships, *Polym. Eng. Sci.* 54 (2014) 840–857.
- [27] Y.-M. Corre, S. Bruzaud, J.-L. Audic, Y. Grohens, Morphology and functional properties of commercial polyhydroxyalkanoates: a comprehensive and comparative study, *Polym. Test.* 31 (2012) 226–235.
- [28] S.b. Charlon, N.g. Follain, E. Dargent, J.r.m. Soulestin, M. Sclavons, S.p. Marais, Poly [(butylene succinate)-co-(butylene adipate)]-montmorillonite nanocomposites prepared by water-assisted extrusion: role of the dispersion level and of the structure-microstructure on the enhanced barrier properties, *J. Phys. Chem. C* 120 (2016) 13234–13248.
- [29] K. Iggui, M. Kaci, M. Mahlous, N.L. Moigne, A. Bergeret, The effects of gamma irradiation on molecular weight, morphology and physical properties of PHBV/cloisite 30B bionanocomposites, *J. Renew. Mater.* 7 (2019) 807–820.
- [30] B. Fei, C. Chen, S. Chen, S. Peng, Y. Zhuang, Y. An, L. Dong, Crosslinking of poly [(3-hydroxybutyrate)-co-(3-hydroxyvalerate)] using dicumyl peroxide as initiator, *Polym. Int.* 53 (2004) 937–943.
- [31] J. Tian, W. Yu, C. Zhou, The preparation and rheology characterization of long chain branching polypropylene, *Polymer* 47 (2006) 7962–7969.
- [32] F. Wu, M. Misra, A.K. Mohanty, Super toughened poly (lactic acid)-based ternary blends via enhancing interfacial compatibility, *ACS Omega* 4 (2019) 1955–1968.
- [33] H. Eslami, M.R. Kamal, Effect of a chain extender on the rheological and mechanical properties of biodegradable poly (lactic acid)/poly [(butylene succinate)-co-adipate] blends, *J. Appl. Polym. Sci.* 129 (2013) 2418–2428.
- [34] S. Trinkle, P. Walter, C. Friedrich, Van Gorp-Palmen Plot II – classification of long chain branched polymers by their topology, *Rheol. Acta* 41 (2002) 103–113.
- [35] M. Avrami, Kinetics of phase change. I general theory, *J. Chem. Phys.* 7 (1939) 1103–1112.
- [36] M. Avrami, Kinetics of phase change. II transformation-time relations for random distribution of nuclei, *J. Chem. Phys.* 8 (1940) 212–224.
- [37] M. Avrami, Granulation, phase change, and microstructure kinetics of phase change. III, *J. Chem. Phys.* 9 (1941) 177–184.
- [38] A. Jeziorny, Parameters characterizing kinetics of nonisothermal crystallization of poly(ethylene-terephthalate) determined by dsc, *Polymer* 19 (1978) 1142–1144.
- [39] T.X. Liu, Z.S. Mo, S.G. Wang, H.F. Zhang, Nonisothermal melt and cold crystallization kinetics of poly(aryl ether ether ketone ketone), *Polym. Eng. Sci.* 37 (1997) 568–575.
- [40] A. El-Hadi, R. Schnabel, E. Straube, G. Müller, S. Henning, Correlation between degree of crystallinity; morphology, glass temperature, mechanical properties and biodegradation of poly(3-hydroxyalkanoate) PHAs and their blends, *Polym. Test.* 21 (2002) 665–674.
- [41] P. Barham, A. Keller, The relationship between microstructure and mode of fracture in polyhydroxybutyrate, *J. Polym. Sci. B Polym. Phys.* 24 (1986) 69–77.
- [42] M. Deroine, A. Le Duigou, Y.-M. Corre, P.-Y. Le Gac, P. Davies, G. César, S. Bruzaud, Accelerated ageing and lifetime prediction of poly (3-hydroxybutyrate-co-3-hydroxyvalerate) in distilled water, *Polym. Test.* 39 (2014) 70–78.
- [43] G.J.M. de Konning, P.J. Lemstra, Crystallization phenomena in bacterial poly [(R)-3-hydroxybutyrate] : 2. Embrittlement and rejuvenation, *Polymer* 34 (1993) 4089–4094.